

Noise Reconstruction and Removal Network: a New Way to Denoise FIB-SEM Image

Katya Giannios¹, Abhishek Chaurasia¹, Guillaume Thibault^{2,4*}, Jessica L. Riesterer^{2,3,4}, Erin S. Stempinski^{2,3}, Terence P. Lo⁴, Bambi DeLaRosa^{1*} and Joe W. Gray^{2,4}

¹ Micron Technology, Inc, Advanced Computing and Emerging Memory Solutions, Boise, ID, United States.

² Dept. of Biomedical Engineering, Oregon Health & Science University, Portland, OR, United States.

³ Multiscale Microscopy Core, Oregon Health & Science University, Portland, OR, United States.

⁴ Knight Cancer Institute, Oregon Health & Science University, Portland, OR, United States.

* Corresponding author: thibault@ohsu.edu, bdelarosa@micron.com

Recent advances in Focused Ion Beam-Scanning Electron Microscopy (FIB-SEM) have led to unprecedented biological tissue visualization and analysis, as well as understanding of cellular ultrastructure and cell-cell interactions [1]. High-resolution FIB-SEM data sets often consist of volumes sliced into thousands of 6K×4K images with 4nm/voxel resolution, allowing a 3D reconstruction of a fraction of tissue volume. Depending on the tissue type, sample preparation, acquisition settings, detector used, etc., the images may contain a significant quantity of noise making any further analysis tedious or even impossible.

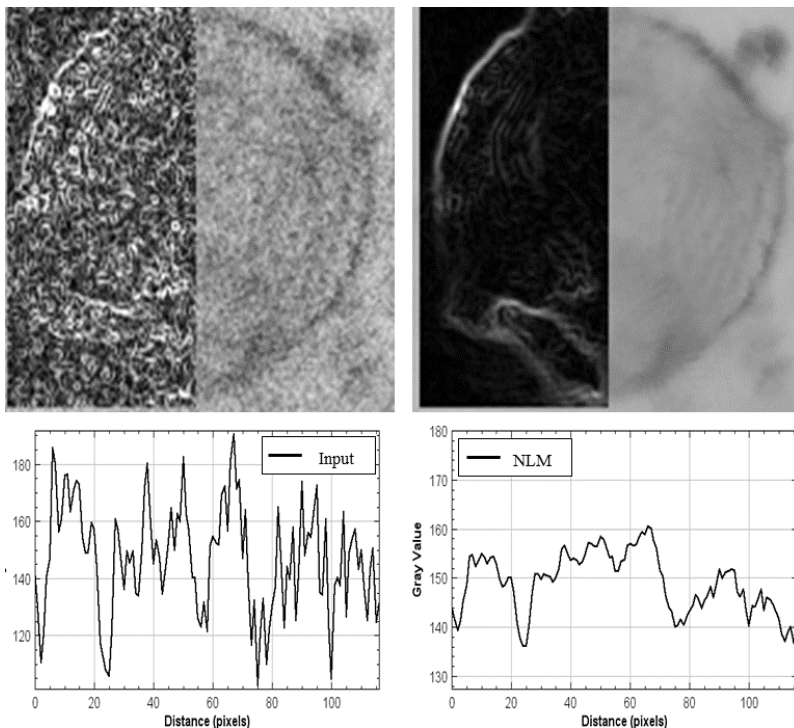
Traditionally for denoising one would look at utilizing BM3D, non-local means (NLM), median or Gaussian filters. In recent years, deep learning methods, and particularly Convolutional Neural Networks (CNNs) have established themselves as powerful analytical tools in data handling - to name just a few [2-7]. In the field of denoising, CNNs have been especially useful [8-10] when the noise characteristics are unknown, making any mathematical modeling difficult. However, these techniques inhabit its own challenges such as providing noise-free images for training. In theory, but not feasible for FIB-SEM imaging, obtaining denoised/like noise-free images is possible by averaging multiple (up to hundreds) acquisitions of the same image.

We propose and further developed the idea of using a sequence of FIB-SEM images with a CNN in an unsupervised training for removing that noise. Our network uses a triplet of images as input and is trained to map one noise realization to the other, using our modified Noise2Noise loss function. We updated the Noise2Noise loss function developed by Wu et al. [13] specifically for denoising a sequence of FIB-SEM images. We refer to the proposed architecture as Noise Reconstruction and Removal Network (NRRN). Fig. 1 shows a visual comparison between our unsupervised NRRN and other state-of-the-art networks trained using supervised techniques. The NRRN is applicable to the case of improving the image quality based on two or three scans of the same slice, or denoising based on the two adjacent slices in the volume stack.

Our approach is to obtain a denoised image from three adjacent noisy images. To do so, we consider the initial tissue sample into a data set of independent triplets of images. We split each triplet into two pairs that are passed through two parallel identical branches of the proposed network NRRN. The neural network architecture uses our novel noise reconstruction module. The design was motivated by ConvLSTM [11] and GRU [12] cells, but with a reduced computational overhead. The module utilizes soft attention and signal boosting that upon deployment on large images (more than 24Mb) homogeneously removes the noise.

We demonstrated on two electron microcopy data sets from different tissue types and collected on different microscopes that this unsupervised approach leads to consistent noise removal across the entire image without regard to the structures present. To that point, we use two classical measures in the evaluation process: the Peak Signal-to-Noise Ratio (PSNR) and the Structural Similarity Index Measure (SSIM). However, we also utilize the interquartile range (IQR) of the signal across a straight line in a flat-signal-area. In our analysis we look at the noise presence in the resin used to fill the space between the cellular structures. The resin is a homogeneous material, and therefore an “efficient” denoiser should produce a flat signal. On a PSNR and SSIM level, our NRRN achieves comparable results to the supervised U-Net [6] and DenoiseNet [14,15]. In the case of NLM, a high PSNR is achieved by aggressively flattening the signal even on biological structures of interest. However, NRRN does a better job in removing noise across the resin while sharpening the biological structures - visible in Fig. 1. NRRN’s architecture paired with our unsupervised training scheme removes the noise and does a better job at preserving the edges of the organelles as compared to U-Net and DenoiseNet, which were trained using supervised techniques.

We also showed that the structure of the NRRN architecture allows a glimpse into the denoising process that can be used to adjust the depth of the network to the available computational resources and/or presence of noise. The detail description of this study and implementation of the code are made publicly available and available upon request.



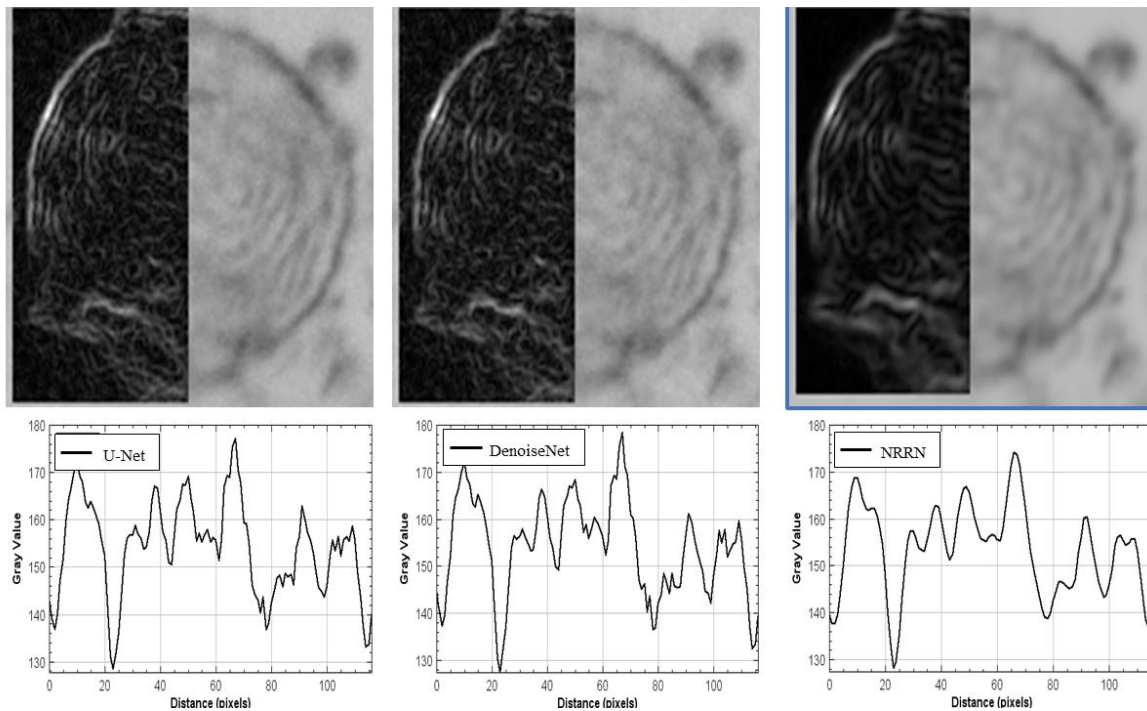


Figure 1: Comparison of the denoising performance (from left to right): Input image, NLM, U-Net, DenoiseNet and NRRN. NRRN's architecture removes the noise and does a better job at preserving the edges of the organelles as compared to Non-local mean, U-Net and DenoiseNet. Top row: right panels raw or denoised image crops, left panels - image being passed through high-pass filter. Bottom row: the signal variation across a straight line.

References:

- [1] CS Xu et al., *Elife* **6** (2017), p. e25916.
- [2] J Redmon and A Farhadi, arXiv preprint (2018), arXiv:1804.02767.
- [3] M Tan, R Pang and QV Le, Proceedings of the IEEE/CVF conference on computer vision and pattern recognition (2020).
- [4] W Sun and Z Chen, *IEEE Transactions on Image Processing*, **29** (2020), p. 4027.
- [5] L-C Chen et al., *Advances in neural information processing systems* (2017).
- [6] O Ronneberger, P Fischer and T Brox, arXiv e-prints (2015), arXiv:1505.04597.
- [7] A Tao, K Sapra and B Catanzaro, arXiv preprint (2020), arXiv:2005.10821.
- [8] D-W Kim, JR Chung and S-W Jung, Proceedings of the IEEE/CVF Conference on Computer Vision and Pattern Recognition Workshops (2019).
- [9] J Liu et al., Proceedings of the IEEE/CVF Conference on Computer Vision and Pattern Recognition Workshops (2019).
- [10] S Yu, B Park and J Jeong, in Proceedings of the IEEE/CVF Conference on Computer Vision and Pattern Recognition (CVPR) Workshops (2019).
- [11] X Shi et al., arXiv e-prints (2015), arXiv:1506.04214.
- [12] K Cho et al., arXiv preprint (2014), arXiv:1406.1078.
- [13] D Wu et al., arXiv e-prints (2019), arXiv:1906.03639.
- [14] T. Remez et al., arXiv e-prints (2017), arXiv:1701.01698.
- [15] T. Remez et al., *IEEE Transactions on Image Processing* **27** (2018), p. 5707.